International Journal of Climatology

International Journal of Climatology RMetS

RESEARCH ARTICLE OPEN ACCESS

Quantifying Multi-Day Precipitation Extremes and Their Linkages With Atmospheric Moisture Flux Over India

T. H. Gaspar[1] | R. M. Trigo[1] | A. M. Ramos[2] | A. S. Raghuvanshi[3] | A. Russo[1,4] | P. M. M. Soares[1] | T. M. Ferreira[1] | A. Agarwal[3]

[1]Universidade de Lisboa, Faculdade de Ciências, Instituto Dom Luiz, Lisboa, Portugal | [2]Institute of Meteorology and Climate Research Troposphere Research (IMKTRO), Karlsruhe Institute of Technology (KIT), Karlsruhe, Germany | [3]Department of Hydrology, Indian Institute of Technology Roorkee, Roorkee, India | [4]CEF – Forest Research Centre, Associate Laboratory TERRA, School of Agriculture,University of Lisbon, Lisbon, Portugal

Correspondence: T. H. Gaspar (thgaspar@fc.ul.pt)

Received: 15 February 2024 | **Revised:** 20 November 2024 | **Accepted:** 4 January 2025

Funding: Financial support by the Portuguese Fundação para a Ciência e a Tecnologia (FCT) I.P./MCTES through national funds (PIDDAC)—UID/50019/2025 and LA/P/0068/2020 (https://doi.org/10.54499/LA/P/0068/2020), project AMOTHEC (https://doi.org/10.54499/DRI/India/0098/2020) and Department of Science and Technology India, DST/INT/Portugal/P-06/2021(G).

Keywords: flash floods | monsoon | multi-day ranking; India | tropical storms

ABSTRACT

The Indian subcontinent is dominated by a very pronounced summer monsoon season from June to September and a less intense autumn monsoon, both posing major challenges to the densely populated regions, namely through flash floods and landslides. Moreover, the spatial patterns and temporal extent of extreme precipitation events are not uniform across India, with event's durations varying across regions and multiple triggering factors. Here, we make use of a high-resolution daily precipitation dataset covering the entire Indian territory, from 1951 to 2022, to analyse multi-day precipitation extremes and their linkages with regional atmospheric moisture fluxes. We consider 10 sub-regions of India, characterised by different climatic regimes and apply an objective ranking of extreme precipitation events, across various time scales, ranging from 1 to 10 days. Obtained results confirm that the method accurately detects and ranks the most extreme precipitation events in each region, providing information on the daily evolution of the magnitude (and spatial extent affected) of high precipitation values in each region. Moreover, results show that top rank events can be associated with different types of storms affecting the four main coastal regions of India. In particular, some top rank events can be critically linked to long duration events (e.g., 10 days) that can be missed in ranks for shorter duration (e.g., 1–3 days) periods, thus stressing the need to employ multi-day precipitation extremes ranking. Finally, an in-depth analysis of the large-scale atmospheric circulation and moisture transport is presented for the top 10-day events influencing the four coastal regions of India. Results show low pressure systems, which persist over multiple days and play a critical role in linking IVT to MDPEs across the Indian subcontinent. Overall, we are confident that our findings are valuable in advancing disaster risk reduction strategies, optimising water resource management practices, and formulating climate change adaptation strategies specifically tailored for the Indian subcontinent.

1 | Introduction

The Indian subcontinent exhibits a wide range of climatic zones and weather phenomena, from tropical in the south to temperate in the north, influenced by geography, monsoon systems, and topography, making it highly diverse climatologically (Guntu et al. 2020; De, Dube, and Prakasa Rao 2005). For instance, the summer monsoon influences the entire subcontinent from June to September, followed up by retreating monsoon in the southern Peninsula of India from October to

December and western disturbance in northern India from December to March. The yearly pattern of monsoon rainfall can be explained as a reflection of the seasonal movement of the Inter-Tropical Convergence Zone (ITCZ) and the consequent transition of rain patterns from the southern to the northern Indian Ocean (Kulkarni et al. 2020). In addition, the Indian subcontinent bears the brunt of nearly 10% of the world's Tropical Cyclones (Dube et al. 2020). Of these, a significant portion originates in the Bay of Bengal, making landfall along the eastern coast of India (Murty, Flather, and Henry 1986). Intense rainfall, often associated with convective systems or cyclonic disturbances lead to flash floods, landslides, and other hydro-meteorological hazards (Mishra and Shah 2018; Ali, Mishra, and Pai 2014). The densely populated regions, particularly in low-lying areas and river basins, are highly vulnerable to the impacts of these extreme events (Srinivas et al. 2010; Singh, Ali Khan, and Rahman 2000). Intense precipitation events and associated risks are expected to occur more frequently in Asian regions, especially in India, Bangladesh, and China (Guntu et al. 2020; Goswami et al. 2006). Extreme precipitation events frequently occur across the Indian subcontinent, particularly during the monsoon season (Raghuvanshi, Trigo, and Agarwal 2025; Sahany et al. 2018; Joseph and Sijikumar 2004; Kumar, Chanda, and Pasupuleti 2020). For instance, extreme precipitation events, exemplified by the Mumbai floods in 2005 and the Kerala floods in 2018, underscore the immense scale of monsoon-associated precipitation events. In 2005, Mumbai was inundated by an unparalleled deluge, inflicting direct economic losses estimated at nearly 2 billion USD and claiming the lives of approximately 500 individuals (Ranger et al. 2010). Similarly, the Kerala floods of 2018 wreaked havoc, causing colossal economic damage, impacting millions of people, and tragically resulting in the loss of over 400 lives (Mishra et al. 2018). Goyal et al. (2022) and Mishra et al. (2018) suggested that climate change may further alter the intensity, duration, and spatial distribution of precipitation events, which could further exacerbate the occurrence of extreme rainfall. A multitude of studies have characterised and ranked precipitation extremes in various parts of the world. Kulkarni et al. (2020) and Kumar, Chanda, and Pasupuleti (2020) have employed various methodologies, including historical analyses and climate models, to understand the drivers and impacts of extreme precipitation in India. These studies have provided valuable insights into the evolving climate dynamics and potential future scenarios of extreme precipitation over the Indian subcontinent. Beguería et al. (2009) used extreme value theory to evaluate the characteristics of extreme precipitation occurrences over north-eastern Iberian Peninsula. An equivalent threshold-based objective method was adopted for identifying regional extreme events while considering their impact area and duration. Ramos, Trigo, and Liberato (2016) proposed a novel approach for ranking daily extreme precipitation based on intensity and areal extent. This method was refined further for multi-day extreme events, using accumulated normalised departure values from climatology at shorter time scales (e.g., 3 days) and longer time scale (e.g., 5, 7, and 10 days) (Ramos et al. 2018). Raj et al. (2021) also adopted similar approach to rank and characterise extreme precipitation events in Indian western Himalayas. However, it is worth mentioning that in some regions and/or different seasons, normalised anomalies of precipitation cannot ensure typical Gaussian distribution. Therefore, this methodology has evolved by employing an alternative upper limit threshold, corresponding to the 95th percentile criterion, in the calculation of extreme precipitation events, akin to the approach proposed by Ramos et al. (2018). Despite the increasing number of publications regarding precipitation extremes, a ranking procedure which accounts for areal extent, intensity, duration and suitable for highly skewed distribution of precipitation has yet to be implemented across the different regions of the Indian subcontinent to assess its robustness. Extreme precipitation is the primary cause of floods, and the mechanisms underlying their intensification in response to a warmer climate are of significant interest (Sorí et al. 2023). The acceleration of the hydrologic cycle driven by climate change, which is mostly attributable to increased atmospheric moisture transport, is largely responsible for this intensification (Mukherjee and Mishra 2021). The fundamental component of the atmospheric branch of the water cycle is atmospheric moisture transport (Gimeno et al. 2012), and variations in this mechanism have a considerable impact on precipitation extremes (Gimeno et al. 2016). During the Indian Summer Monsoon (ISM), the majority of atmospheric moisture is transported through surface to mid-tropospheric levels from the Arabian Sea and southern Indian Ocean across the equator (Patil et al. 2018). According to Cadet and Greco (1987), the majority (70%) of moisture transport reaches the west coast of India from the Southern Indian Ocean through the Somali low-level jet while the remaining moisture (30%) arises from the Arabian Sea through evaporation. The complete identification of the major sources of moisture affecting the India continent (and all the regions of the world) has been improved with the use of robust Lagrangian models (Gimeno et al. 2012). During the withdrawal of ISM, low-level winds over India change their direction from southwest to northeast. The continental tropical convergence zone and the subtropical anticyclone's (anticyclone) southward shift are linked to this change (Rajeevan et al. 2012). The India Meteorological Department (IMD) refers to the October to December period as the northeast monsoon, which is a part of the northeast trades (Rajeevan et al. 2012). The region receives roughly 11% of its annual rainfall during the northeast monsoon season, whereas certain regions throughout the south peninsula (Deccan Plateau & Eastern Ghats) receive between 30% and 60%. The northeast monsoon rainfall's inter-annual fluctuation affects many different industries, including agriculture and the south of peninsular India's water supplies (Rajeevan et al. 2012). A wide range of indices have been developed to measure the movement of moisture in the atmosphere. Many studies have previously used column integrated water vapour (IWV) data obtained from microwave sensors because satellite images of water vapour that are easily accessible (Neiman et al. 2008). In addition, the column integrated water vapour transport (IVT), which includes horizontal winds in its computation, has become the standard metric to assess moisture advection. Two further advantages of IVT over IWV are its capacity to identify stronger correlations more accurately with precipitation and that it is better predicted at longer time leads by numerical weather prediction models. The relationship between atmospheric moisture transport and extreme precipitation and floods in India has been shown in several previous studies

(Dhana Laskhmi and Satyanarayana 2020; Lyngwa and Nayak 2021; Goyal et al. 2022; Mahto et al. 2023; Raghuvanshi and Agarwal 2023; Raghuvanshi and Agarwal 2024). The bulk of these studies, however, is concentrated on understanding the atmospheric moisture transport linked to intense precipitation events that persisted for shorter periods of time (e.g., up to 3 days). Our study addresses a gap by analysing multi-day precipitation extremes linked to regional atmospheric patterns, which are often tied to IVT. These patterns, covering spatial scales of approximately 1000 km and lasting from several days to a week, play a crucial role in forecasting and understanding extreme weather events (Raghuvanshi and Agarwal 2023). Under certain synoptic conditions, anomalous moisture transport via IVT can result in prolonged heavy precipitation, potentially leading to severe flooding with significant socio-economic consequences (Ramos et al. 2018; Slinskey et al. 2020). This study aims to develop objective rankings of extreme precipitation in India, considering events across different time scales, ranging from daily to 10-day durations. These rankings are produced for different spatial aggregations, encompassing the entire Indian subcontinent. By considering multi-day extreme precipitation events, the study highlights the distinct implications of shorter-duration heavy rainfall events (associated with flash flooding) and longer-duration events (linked to large-scale flooding and other disruptive consequences). The identification of extreme precipitation events across various time scales will allow us to enhance the current understanding of the temporal progression and regional variability of floods in the subcontinent. This paper is structured as follows: Section 2 covers the data used and the methodology employed, Section 3 displays the results, and Section 4 provides a summary of the key finding and conclusions.

2 | Data and Methodology

2.1 | Dataset and Regions

In the current study the India Meteorological Department daily gridded precipitation dataset for the Indian mainland (between $68°E - 98°E$ and $8°N - 37°N$) is used (Pai et al. 2014). The dataset consists of accumulated daily precipitation (mm) and offers a remarkably high spatial resolution of $0.25° \times 0.25°$. To create this gridded dataset, a comprehensive network of 6995 gauging stations located throughout India was utilised. The daily data includes a period of 71 years (1951–2022). Over time, numerous research studies have used this dataset, revealing its broad applicability and reliability. These studies have covered a wide range of topics, such as exploring the spatiotemporal variability of precipitation (Guntu et al. 2020; Sahany et al. 2018), conducting extreme precipitation analyses (Ali, Mishra, and Pai 2014; Vinnarasi and Dhanya 2016), investigating the intrinsic predictability of Indian precipitation (Guntu et al. 2020; Mishra and Shah 2018), and examining the spatial diversity of Indian precipitation teleconnections (Kurths et al. 2019), among others. Across diverse studies, the consistent use of the IMD gridded dataset confirms its high accuracy and robustness in capturing India's precipitation distribution. This dataset has proven invaluable to researchers from various fields, enhancing our understanding of regional precipitation patterns and trends (Pai et al. 2021). Its wide-ranging applications have bolstered its credibility and reliability, making it a vital tool for addressing scientific questions related to Indian climate and meteorology (Raj et al. 2021).

The climate of India exhibits significant spatial diversity characterised by distinct topography and types of climates; with the local precipitation distribution presents a wide range of skewness values (Figure S1). Therefore, dividing the Indian subcontinent into homogeneous precipitation regions is considered essential before ranking the extreme precipitation events. The climate of India exhibits significant spatial diversity due to its vast geography and varied topography. This spatial variability in precipitation adds complexity to the study of hydrological extremes such as floods and droughts. Given this diversity, previous research has emphasised the importance of investigating hydrological extremes at homogeneous regions scale. Previous studies Bharath and Srinivas (2014); Mannan et al. (2017) have attempted to quantify India's homogeneous precipitation regions based on various precipitation characteristics such as mean, magnitude, skewness, and standard deviation. The Indian Meteorological Department (IMD) has historically defined homogeneous regions to facilitate such analyses. However, existing literature found that these regions fall short for representing coherent climate conditions. This is primarily because they do not account for the temporal variability that characterises precipitation patterns in India. Temporal variability refers to how precipitation patterns change across different time scales, from daily and seasonal cycles to inter-annual fluctuations. Accounting both magnitude and temporal variability of precipitation is crucial for robust identification of homogeneous regions. Despite the recognition of these shortcomings, there remains a research gap in explicitly including temporal variability within the framework for developing homogeneous zones. Addressing this gap, Guntu et al. (2020) proposed a novel method for precipitation regionalization using a self-organising map coupled with a multi-scale standardised variability index. The time series of gridded precipitation at different time scales is selected as a clustering variable. This means that homogeneous regions are defined based on coherent climate variability at different time scales (monthly, seasonal, and annual) rather than mean climate conditions. Given this, Guntu et al. (2020) suggested partitioning the Indian subcontinent into 10 distinct regions (Figure 1), that is, Western India (WI), North-western India (NWI), North-central India (NCI), Eastern India (EI), South-central India (SCI), South-eastern coastline (SEC), Konkan coast (KC), North-eastern India (NEI), Rain-belt Western Himalaya (RBWH) and Rain-shadow Western Himalaya (RSWH).

Furthermore, we used the European Centre for Medium-Range Weather Forecasts (ECMWF) version 5 reanalysis (ERA5), known for its high spatiotemporal resolution on a global scale (Hersbach et al. 2020). Based on comparative analyses with other reanalysis products, recent research have shown that ERA-5 is appropriate for meteorological and hydrological assessments in the Indian subcontinent (Dullaart et al. 2021; Mahto et al. 2023). The spatial resolution of the ERA5 latitude-longitude grid is $0.25° \times 0.25°$. We retrieved specific humidity and horizontal wind fields (zonal and meridional wind speed) at multiple vertical levels of the troposphere (1000–300 hPa; 20 pressure levels total) at a 6-hourly temporal resolution to quantify atmospheric

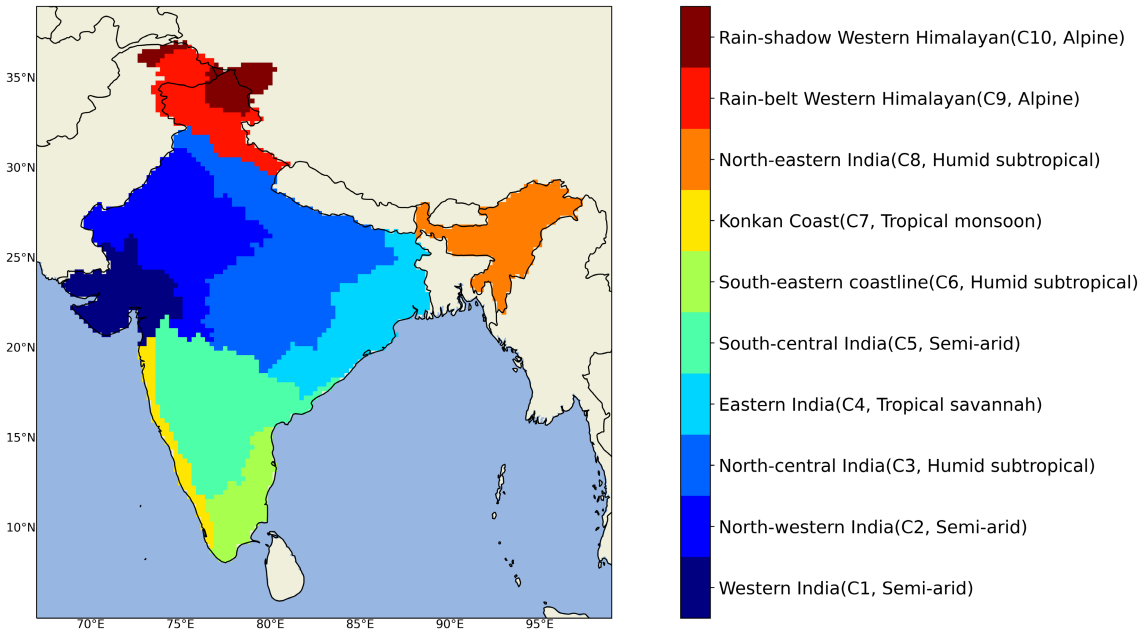

FIGURE 1 | Sub-regions of the Indian mainland. Each region's name is displayed, and the type of climate regime is listed in parentheses. [Colour figure can be viewed at wileyonlinelibrary.com]

moisture transport. Additionally, mean sea level pressure (MSLP), temperature at 850, 500 hPa (T850 and T500, respectively) and geopotential height at 850, 500 hPa (Z850 and Z500, respectively) were retrieved at 6 hourly temporal resolutions to investigate regional atmospheric patterns.

2.2 | Ranking Extreme Precipitation Method

We ranked extreme precipitation events using the methodology developed by Ramos et al. (2018). This ranking method considers magnitude, spatial extent and duration of the extreme precipitation events. For the ranking estimation, only wet days (i.e., days with precipitation greater than 1 mm) are considered. A four-step procedure is used to determine the ranks of extreme precipitation events across multi-day accumulation periods (schematic representation in Figure S2). First, we perform the computation of accumulated precipitation over various time intervals, ranging from daily to 10-day periods. Subsequently, to rank extreme precipitation events, we utilise the precipitation departures from the 95th percentile climatology of each accumulated precipitation period. Then, for each day and at grid point, a measure of event magnitude is determined as follows:

$$N95_{(p,d,i,j)} = \text{acc\_precipitation}_{(p,d,i,j)} - \text{P95th}_{(p,t,i,j)} \quad (1)$$

- The P95th (p,t,i,j) is the 95th percentile of the accumulated precipitation dataset over a certain period (p) for that particular grid point (i,j) and Julian day (t);
- acc_precipitation (p,d,i,j) is the accumulated precipitation, corresponding to the day (d) over certain period (p), and grid point (i,j);
- N95 (p,d,i,j) is the extreme anomalous precipitation for the day (d) over the accumulated period (p), at the grid point (i, j).

The 95th percentile threshold was computed for each grid point, for each Julian day (t) and for each accumulated precipitation period (p), ensuring a fair analysis across all grid points. This methodology allows for the characterisation of each day, considering not only the severity of the precipitation but also the associated spatial extension within the 10 regions identified previously (Figure 1). For example, the extreme anomalous precipitation for the 28 November 2008 over the accumulated period of 3-days (N95_(p,d,i,j); $p = 3$-days; $d = 28$ November 2008) corresponds to the accumulated precipitation during 26–28 November 2008 (acc_precipitation_(p,d,i,j), where $p = 3$-days and $d = 28$ November 2008) minus the 95th percentile for the accumulated precipitation dataset for the period of 3-days and for the corresponding Julian day(prec_95th percentile_(p,t,i,j); $p = 3$-days, $t = 28$ November). The calculation of the local percentiles encompassed the complete reference period available spanning from 1951 to 2022. However, as stated above, this procedure was restricted to days with a minimum daily precipitation threshold of 1 mm (referred to as wet days). This restriction ensures that only days with precipitation are considered in the computation. Our focus lies in regions where precipitation exceeds the 95th percentile (positive anomalies). To determine the magnitude of an event (hereafter R), a daily calculation is performed by multiplying two factors:

$$R = A^{*}M \quad (2)$$

- The area (referred to as A, represented as a percentage) exhibiting precipitation anomalies (N95(p,d,i,j)) greater than zero, and
- The mean value of these anomalies (referred to as M) across all grid points characterised by precipitation anomalies greater than zero.

After we compute the magnitude (R) of each precipitation extreme event over the 10 distinct regions in Figure 1, we ranked

the most extreme ones and this resulted in a total of 50 different rankings, considering various accumulation periods (daily, 3, 5, 7, and 10 days) across the 10 domains. To establish a common understanding, the following terminology is adopted:

- "Case" refers to an individual accumulation associated with each specific ranking.
- "Event" represents a collection of cases, which can be present in the same accumulation ranking or across different accumulation rankings for each domain.

To keep the analysis manageable and highlight key features of the multi-daily rankings, we will focus solely on the results obtained for the four main coastal regions of the Indian subcontinent (Western India (C1), Eastern India (C4), South-eastern coastline (C6), and Konkan coast (C7); Figure 1), as we seek to establish a potential relationship with water vapour plumes. It is important to emphasise that the position within the ranking is independent of whether significant socioeconomic impacts occur or not.

2.3 | Integrated Water Vapour Transport (IVT)

The IVT, also known as atmospheric moisture transport or moisture flux, is calculated using zonal (u; m/s) and meridional (v; m/s) wind components, as well as specific humidity (q; kg/kg) at various adjacent pressure levels, ranging from 1000 to 300 hPa, within the Eulerian framework (Neiman et al. 2008; Lavers et al. 2012) using the following equation:

$$\begin{aligned} IVT &= \sqrt{IVT_x^2 + IVT_y^2} \\ &= \sqrt{\left(\frac{1}{g}\int_{1000}^{300} qu\,dp\right)^2 + \left(\frac{1}{g}\int_{1000}^{300} qv\,dp\right)^2} \end{aligned} \tag{3}$$

where q is the layer-averaged specific humidity $\left(\mathrm{Kg\,Kg^{-1}}\right)$; u and v are the layer averaged zonal and meridional winds $\left(\mathrm{ms^{-1}}\right)$, respectively; g is the acceleration due to gravity; and dp is the pressure difference between two adjacent pressure levels. It is worth stressing that disregarding the levels above 300 hPa will have negligible influence on the output, since water vapour is largely concentrated in the lower troposphere (Zhou and Ru-Cong 2005; Payne and Magnusdottir 2014).

3 | Results and Discussion

To illustrate the functionality of the multi-day ranking system (1, 3, 5, 7, and 10 days) for the four main coastal regions of the Indian subcontinent (Western India (C1), Eastern India (C4), the South-eastern coastline (C6), and the Konkan coast (C7); as shown in Figure 1), we highlight the most noteworthy instances of extreme precipitation events detected through our methodology. These examples correspond to the top events in the selected regions and accumulated periods considered. All selected events described below have produced considerable socio-economic impacts.

3.1 | Multi-Day Ranking

3.1.1 | Konkan Coast (C7)

The Konkan coast, located along the western state of Maharashtra, experiences distinct precipitation patterns due to its proximity to the Arabian Sea and its geographical features. The region is primarily affected by the Southwest Monsoon, which occurs from June to September, bringing most of the annual rainfall (Guhathakurta et al. 2014). The first case, ranked as the top one, in the 3-day accumulated precipitation ranking for the Konkan coast, corresponds to August 4, 2004 (Figure 2a). As previously mentioned, this case represents the accumulated normalised precipitation anomalies between August 2 and August 4, 2004. During these 3 days, there were extreme precipitation anomalies exceeding 200 mm observed over the north-Konkan coast, as indicated by the solid black contour line in Figure 2a.

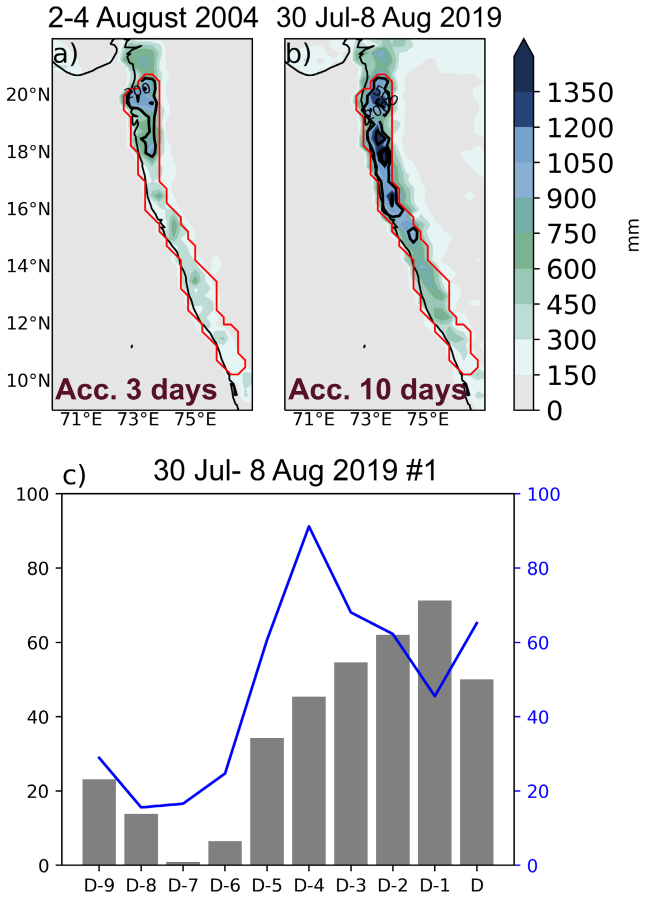

FIGURE 2 | (a) Three days accumulated precipitation (mm, shaded) and corresponding extreme precipitation anomalies (black contour) of the first most anomalous (3 days ranking) case in Konkan coast: 2–4 August 2004; (b) 10 days accumulated precipitation (mm, shaded) and corresponding extreme precipitation anomalies (black contour) of the #1 case in Konkan coast: 30 July–8 August 2019; (c) The percentage of area with positive anomalies (bars) and the respective anomalies mean (blue line) between 30 July and 8 August 2019 is also shown for the Konkan coast domain. [Colour figure can be viewed at wileyonlinelibrary.com]

In this region, a total of 1000 mm of rainfall was recorded for the 3-day accumulated period.

In August 2019, the Konkan coastal region (C7) experienced severe flooding due to heavy and persistent rainfall resulting in significant impacts on the population and infrastructure (Vijaykumar et al. 2021). This event was considered the most extreme event (1) in the 10-day accumulated precipitation ranking corresponding to August 8, 2019. This day appears also for the 3-day accumulated precipitation ranking (8), and #6 for the 5, and 7-day accumulated precipitation rankings, respectively. Figure 2b shows totals above 1500 mm recorded for the 10-day accumulated period over the north-Konkan coast. Extreme precipitation anomalies above 200 mm were recorded from the 16° N latitude to the northeast part of this region, reaching anomalies of 500 mm over the northeast part of Mumbai (Figure S4).

Figure 2c displays the individual day ranking metrics [A (grey bars) and M (blue line)] which allows us to analyse the 10-day accumulated precipitation anomalies, and the area affected between 30 July and 8 August 2019 (10-days period). A substantial increase in the area with positive anomalies is observed, starting on August 2 and peaking on August 7. The mean value of these anomalies exhibits a similar trend but reaches its highest value earlier on August 4. The top nine cases for the 10-day accumulated precipitation for the Konkan coast are summarised in Figure S3.

The meteorological assessment conducted by Vijaykumar et al. (2021) shows the presence of a mesoscale cloudburst event over Kerala between 8 and 22 UTC on August 8, 2019. The heavy rainfall led to overflowing rivers, waterlogging in low-lying areas, and landslides in the hilly regions (Vijaykumar et al. 2021). Several towns and villages along the coast were affected, and there were reports of damage to infrastructure, homes, and agricultural land (a20, 2020).

According to the International Disaster Database (EM-DAT), which encompasses data on the occurrence and impacts of over 26,000 mass disasters worldwide from 1900 to the present day, the Konkan coast and Western India regions suffered 1900 fatalities and affected approximately 3,000,000 individuals during the summer period. The database is meticulously compiled from diverse sources, including UN agencies, non-governmental organisations, reinsurance companies, research institutes, and press agencies. Although the considered period extends beyond the 10 days examined here, a substantial fraction of the total casualties mentioned can be attributed to the August 2019 event.

Figure 3 illustrates the top ten extreme precipitation events for the Konkan coast over various durations (1, 3, 5, 7, and 10 days). The results reveal that many occurrences, which are not significant on a daily basis, become substantial over longer periods based on intensity and spatial extent. Notably, the August 2019 event stands out and occupies most top positions, particularly for longer accumulated precipitation scales like the 10-day period, where it accounts for 9 out of the first 10 positions but is ranked in a lower position for the 1-day ranking. Similarly, the august 2004 event appears in the 3-day ranking category but is ranked low for the 1 and 5 day accumulated period (Figure 3; Tables S1 and S2). These differences in rankings across different durations highlight the importance of ranking extreme precipitation events to capture events with varied spatiotemporal characteristics. Additionally, Overall, Figure 3 shows that the top ranks for different durations are dominated by the august 2019 event. It is important to emphasise that analysing longer temporal scales introduces some inertia, resulting in certain events occupying multiple positions in corresponding rankings over successive periods. This phenomenon is particularly evident for the Konkan coast (Figure 3), where we can observe that the August 2019 event notably stands out, dominating most top positions, especially in longer accumulated precipitation scales such as the 10-day period, where it holds 9 out of the first 10 positions event also appears frequently in the top rankings.

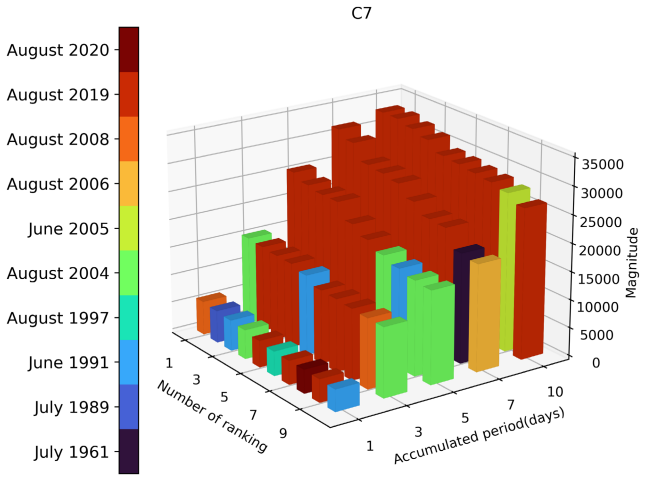

FIGURE 3 | The top ten events for each different anomalous accumulated precipitation rankings (1, 3, 5, 7, and 10 days) for the Konkan coast domain. [Colour figure can be viewed at wileyonlinelibrary.com]

3.1.2 | Western India (C1)

Western India experiences a diverse range of precipitation characteristics due to its vast geographical extent, ranging from coastal areas to more arid inland regions. The state's precipitation patterns are influenced by the southwest monsoon, local weather systems, and the Arabian Sea (Guntu et al. 2020; Guhathakurta et al. 2014). Here we analyse the most extreme precipitation events for the 3-day (27–29 July 2015, Figure 4a) and 10-day (July 4, 2005, Figure 4b) accumulated periods in the Western India region.

During the 3-day event (spanning from July 27 to July 29, 2015), the accumulated precipitation surpassed 500 mm over a considerable area, with the maximum value reaching around 900 mm in the north of Ahmedabad city (Figure 4a). The In contrast, the first event in the ranking for the 10-day accumulated period took place on July 4, 2005. During this period, the 10-day accumulated precipitation in Mumbai and its northern regions exceeded 900 mm (Figure 4b). The sheer volume of rainfall in such a short span of time led to extensive flooding and waterlogging in various areas. In July 2005, the city of Mumbai, also known as Bombay, suffered catastrophic floods caused by intense and prolonged rainfall during the monsoon season. The Mumbai municipal area was severely affected by flash floods and landslides,

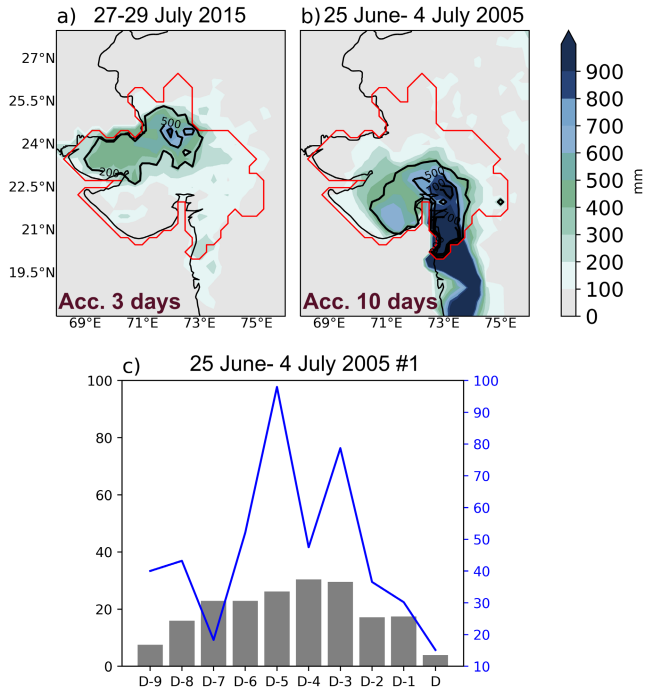

FIGURE 4 | (a) Three days accumulated precipitation (mm, shaded) and corresponding extreme precipitation anomalies (black contour) of the first most anomalous (3 days ranking) case in Western India: 27–29 July 2015; (b) 10 days accumulated precipitation (mm, shaded) and corresponding extreme precipitation anomalies (black contour) of the #1 case in Western India: 25 June- 4 July 2005; (c) The percentage of area with positive anomalies (bars) and the respective anomalies mean (blue line) between 25 June and 4 July 2005 is also shown for the Western India domain. [Colour figure can be viewed at wileyonlinelibrary.com]

resulting in a tragic loss of life. According to reports, at least 419 individuals lost their lives due to the calamity. Additionally, another 216 fatalities were attributed to flood-related illnesses.

The catastrophe also wrought havoc on the region's infrastructure, with over 100,000 residential and commercial establishments damaged, along with approximately 30,000 vehicles (Gupta 2007). According to Gupta (2007), these floods constituted one of the most severe natural disasters in the city's history, resulting in significant impacts on infrastructure, transportation, and the well-being of its inhabitants. The percentage of areas with positive values of N95 (Equation (1)) at the daily scale remains essentially between 20% and 40% range from June 25 to July 4, 2005 (Figure 4c). The daily average of the anomaly (blue line) for this period and region fluctuates significantly, reaching its peak on 29 June (denoted as D-6 in Figure 4c). Daily precipitation (mm, shaded) and corresponding standard deviation anomalies (black contour) between 25 June 2005 and 4 July 2005 are shown in Figures 5 and S5. The most intense days of precipitation were observed on the 28, and 29 of June and 1 July, while the last day of this event (4th July) does not reveal significant precipitation. Over these days' precipitation reached values above 300 mm mostly over the center and south part of western India (Figure 5). Overall, these figures highlight once again the importance of studying precipitation extremes at different timescales to differentiate between extreme precipitation events that occur daily and those that affect a particular region through successive days. Examining these different timescales allows for a better understanding of the characteristics and impacts of extreme precipitation, contributing to more accurate assessments of regional climate variability and potential flood risks.

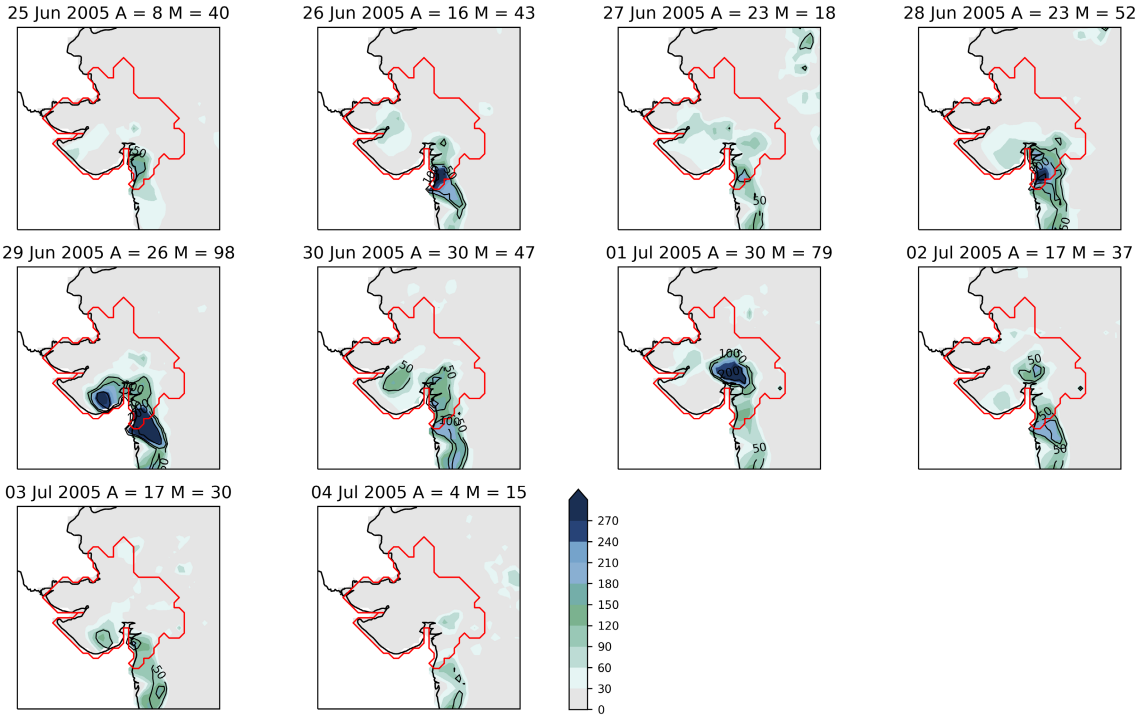

FIGURE 5 | Daily precipitation (mm, shaded) and corresponding standard deviation anomalies (black contour) between 25 June 2005 and 4 July 2005 of the most extreme case for the 10-day accumulated period over Western India (C1). [Colour figure can be viewed at wileyonlinelibrary.com]

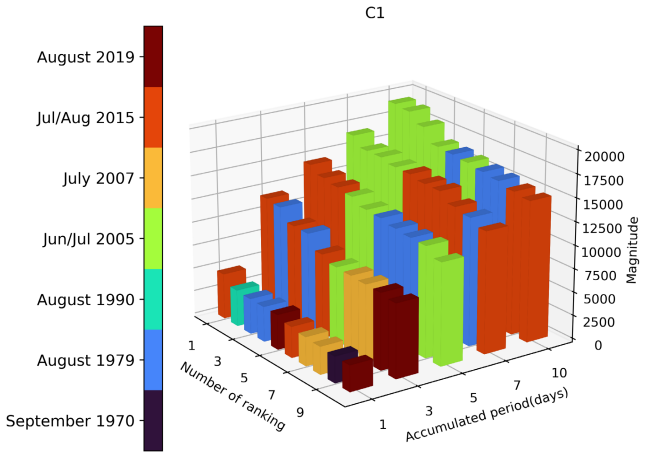

FIGURE 6 | The top ten events for each different anomalous accumulated precipitation rankings (1, 3, 5, 7 and 10 days) for the Western India domain. [Colour figure can be viewed at wileyonlinelibrary.com]

Figure 6 illustrates the top ten extreme precipitation events for Western India over various accumulated periods (1, 3, 5, 7, and 10 days). The results reveal that the 2015 and 2005 episodes dominate the rankings for the 3, 5, 7, and 10-day periods but rank lower for the 1-day period (Tables S1 and S2). These differences in rankings across different durations highlight the importance of applying this methodology to capture events with varied spatiotemporal characteristics.

3.1.3 | South-Eastern Coastline (C6)

The precipitation in this area is mostly influenced by cyclonic systems, and the autumn northeast monsoon (Lyngwa and Nayak 2021; Srinivas et al. 2010). According to our results, 28 November 2008 holds the top position in the rankings for both the 3-day and 10-day accumulated extreme precipitation periods (Figure 7a,b). This event is associated with the passage of Cyclone "Nisha," which formed in the Indian Ocean region at the end of November. Originating as a low-pressure system over Sri Lanka, it gradually intensified into a tropical cyclonic storm.

According to Srinivas et al. (2010), the tropical cyclone moved slowly and made landfall near Karaikal, affecting the Southeastern coast. This led to heavy rainfall, severe flooding, and the loss of 78 lives, along with significant crop damage. Notably, "Nisha" remained quasi-stationary near the coast for about 24 h, causing exceptionally heavy rainfall. Our assessment indicates that for the 10-day cumulative duration, strong precipitation was registered across the entire western zone (Figure 7b), with values exceeding 900 mm in the city of Thanjavur. The aggregated daily analysis (Figure 7c) shows that until 23 November 2008 there was a minimal amount of precipitation. However, starting from November 24th, a huge increase both in the area with positive anomalies and the corresponding average of these anomalies is seen, meaning that those the precipitation that fell during those confirmed by Figures S6 and S7, where it is displayed the corresponding precipitation and standard deviation anomalies, at the daily scale, between November 19 and November 28, 2008.

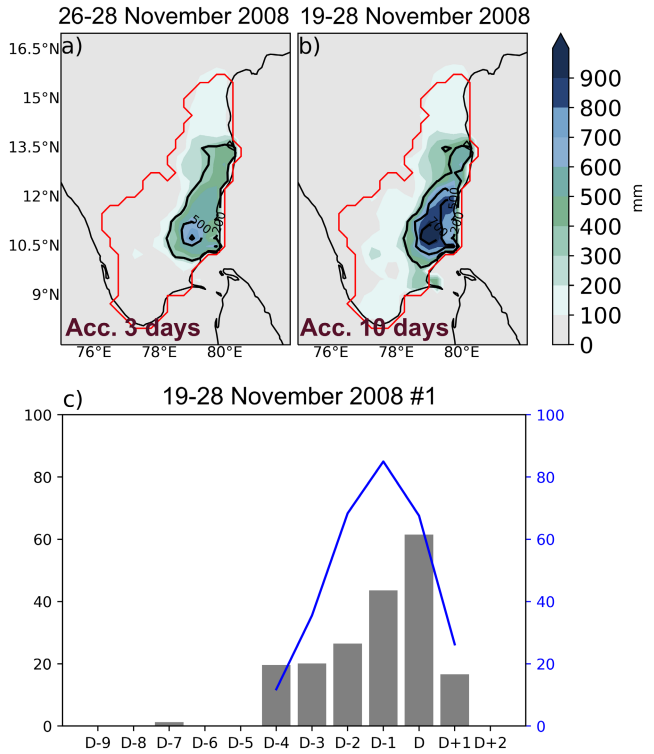

FIGURE 7 | (a) Three days accumulated precipitation (mm, shaded) and corresponding extreme precipitation anomalies (black contour) of the first most anomalous (3 days ranking) case in South-eastern coastline: 26–28 November 2008, (b) 10 days accumulated precipitation (mm, shaded) and corresponding extreme precipitation anomalies (black contour) of the #1 case in South-Eastern coastline: 19–28 November 2008. (c) The percentage of area with positive anomalies (bars) and the respective anomalies mean (blue line) between 19 November and 30 November 2008 is also shown for the South-eastern coastline domain. [Colour figure can be viewed at wileyonlinelibrary.com]

Figure 8, along with Tables S1 and S2, displays the top ten events ranked by anomalous accumulated precipitation over the southeastern coastline region. Accordingly, the top ten positions for the 5, 7, and 10-day accumulated extreme precipitation rankings clearly indicate a significant dominance of the late November and early December 2008 event. In any case, this event is clearly the most extreme (1) event over all accumulated rankings.

3.1.4 | Eastern India (C4)

The Eastern India region is influenced by both the summer South-West Monsoon and the autumn North-East Monsoon, resulting in distinct rainfall patterns throughout the year (KHOLE and DE, 2003; Soman and Kumar 1990). The top rank positions for the 3-day and 10-day rankings correspond to the 4 July 2006 and the 17 May 1995 events, are shown in Figure 9. Notably, the precipitation patterns in the region exhibit distinct characteristics for each event. The 3-day top-ranked event shows accumulated precipitation predominantly concentrated in an "inland" sector of the Orissa region, with precipitation levels ranging from 300 to 500 mm (Figure 9a). According to EM-DAT, the July 2006 event was due to monsoon mechanism, and it was responsible for 33 fatalities. In

contrast, the leading event in the 10-day accumulated period reveals much larger precipitation amounts near the shore, encompassing a larger geographical area and reaching values above 500 mm (Figure 9b). When looking into the daily precipitation evolution (Figures S8 and S9), it is evident that the largest precipitation contribution for the 10-day accumulated period for the May 1995 event occurred between May 10 and 11. The concentrated area of significant precipitation was primarily observed over the coastal southwest sector of the region during these 2 days. Additionally, noteworthy precipitation was recorded over the Northeast littoral area on May 16.

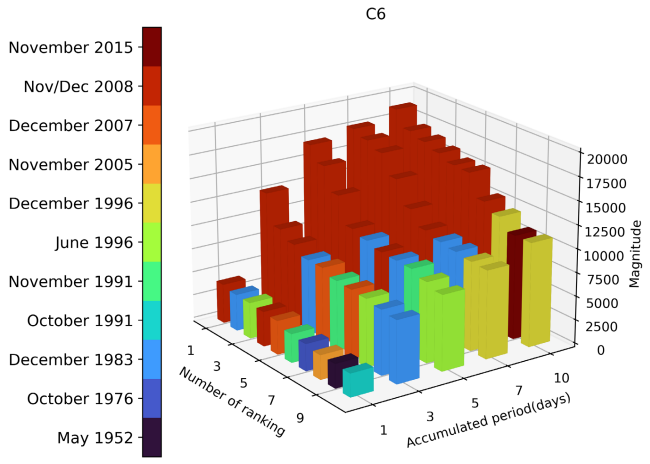

FIGURE 8 | The top ten events for each different anomalous accumulated precipitation rankings (1, 3, 5, 7 and 10 days) for the Southeastern domain. [Colour figure can be viewed at wileyonlinelibrary.com]

When analysing the top ten events over the Eastern India region (Figure 10). Inference can be drawn that numerous cases, especially for the 5-day, 7-day, and 10-day periods, correspond to relatively older events (e.g., May 1995, October 1978, and September 2000). More recent occurrences (October 2013 and July 2006) only rank higher positions for the daily and 3-day periods.

It is important to note that despite these high precipitation values, they remain significantly below the corresponding top-ranking values for the Konkan coast (Figure 3) or Western India (Figure 6). This indicates that the distribution and intensity of rainfall events vary considerably across different geographical locations.

3.2 | Seasonal Distribution of Extreme Events

We analysed the seasonal distribution of the top 100 cases in the ranking for all time periods across the four coastal regions defined previously (Figure 11). Our results indicate that the

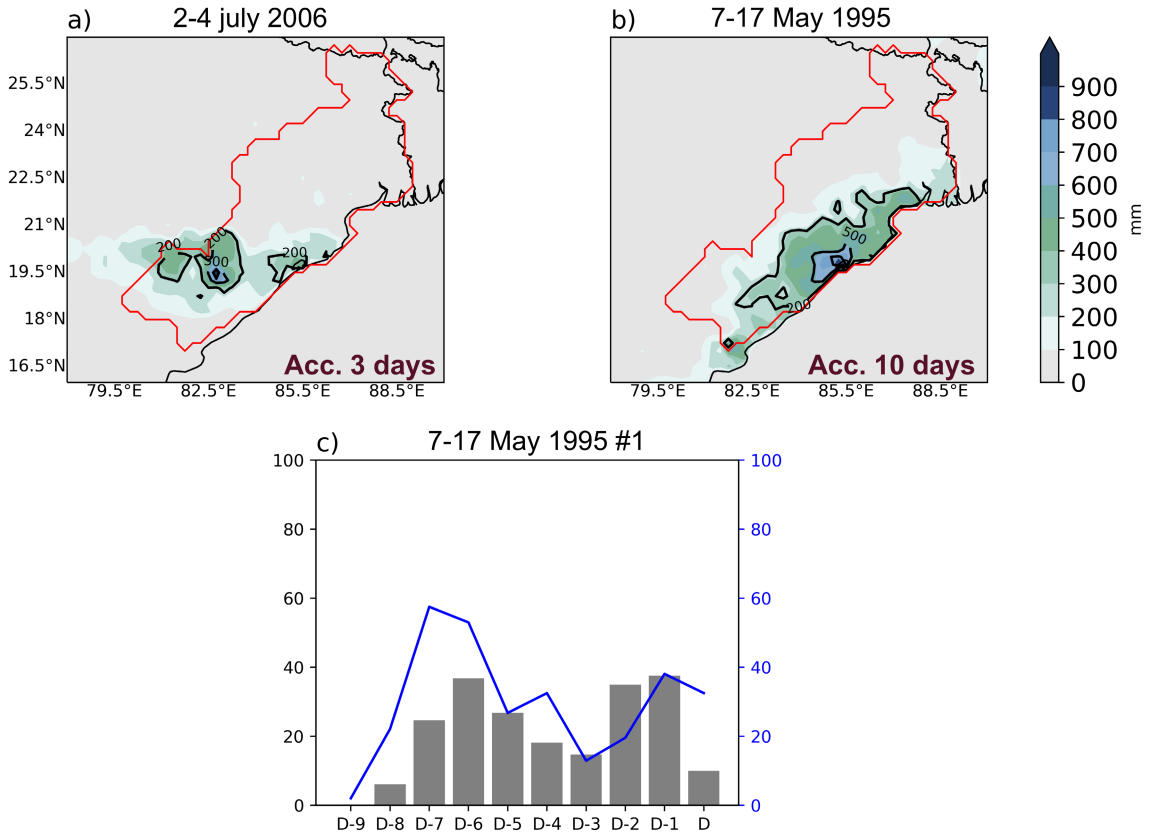

FIGURE 9 | (a) Three days accumulated precipitation (mm, shaded) and corresponding extreme precipitation anomalies (black contour) of the first most anomalous (3 days ranking) case in Eastern India: 2–4 July 2006; (b) 10 days accumulated precipitation (mm, shaded) and corresponding extreme precipitation anomalies (black contour) of the #1 case in Eastern India: 7–17 May 1995; (c) The percentage of area with positive anomalies (bars) and the respective anomalies mean (blue line) between 7 May and 17 May 1995 is also shown for the Eastern India domain. [Colour figure can be viewed at wileyonlinelibrary.com]

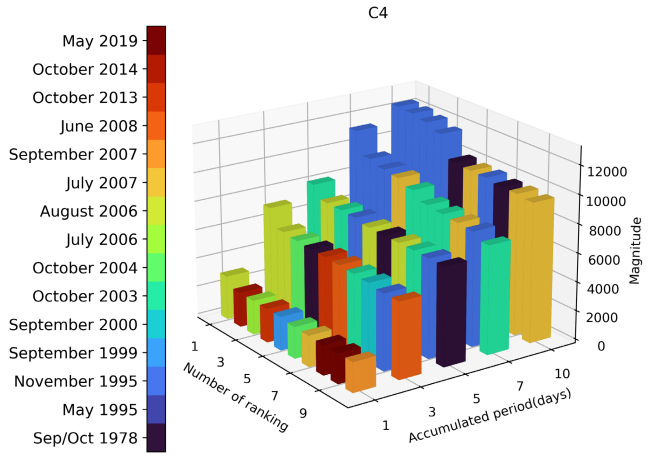

FIGURE 10 | The top ten events for each different anomalous accumulated precipitation rankings (1, 3, 5, 7 and 10 days) for the Eastern India domain. [Colour figure can be viewed at wileyonlinelibrary.com]

highest-ranked extreme precipitation events predominantly occur from June to September, with a peak in August in the Western and Konkan regions (Figure 11a,b). This finding underscores the significant role of the Indian summer monsoon, which contributes about 60%–90% of the annual precipitation in these areas (Joseph and Sijikumar 2004; Guhathakurta et al. 2014; Sahany et al. 2018; Kulkarni et al. 2020). In the South-eastern coastline (C6), the seasonal distribution of precipitation occurrences reveals two distinct maxima (Figure 11c). The first peak occurs in May and June, likely linked to the Indian summer monsoon onset over the southwestern tip of the Indian peninsula in early June or to cyclonic systems prevalent in the pre-monsoon months of April, May, and June. The second peak, with the highest precipitation occurrences from October to December, is largely influenced by tropical cyclonic systems and the northeast monsoon, which is typically active during these months (Srinivas et al. 2010; Lyngwa and Nayak 2021). In Eastern India (C4), the seasonal distribution shows major

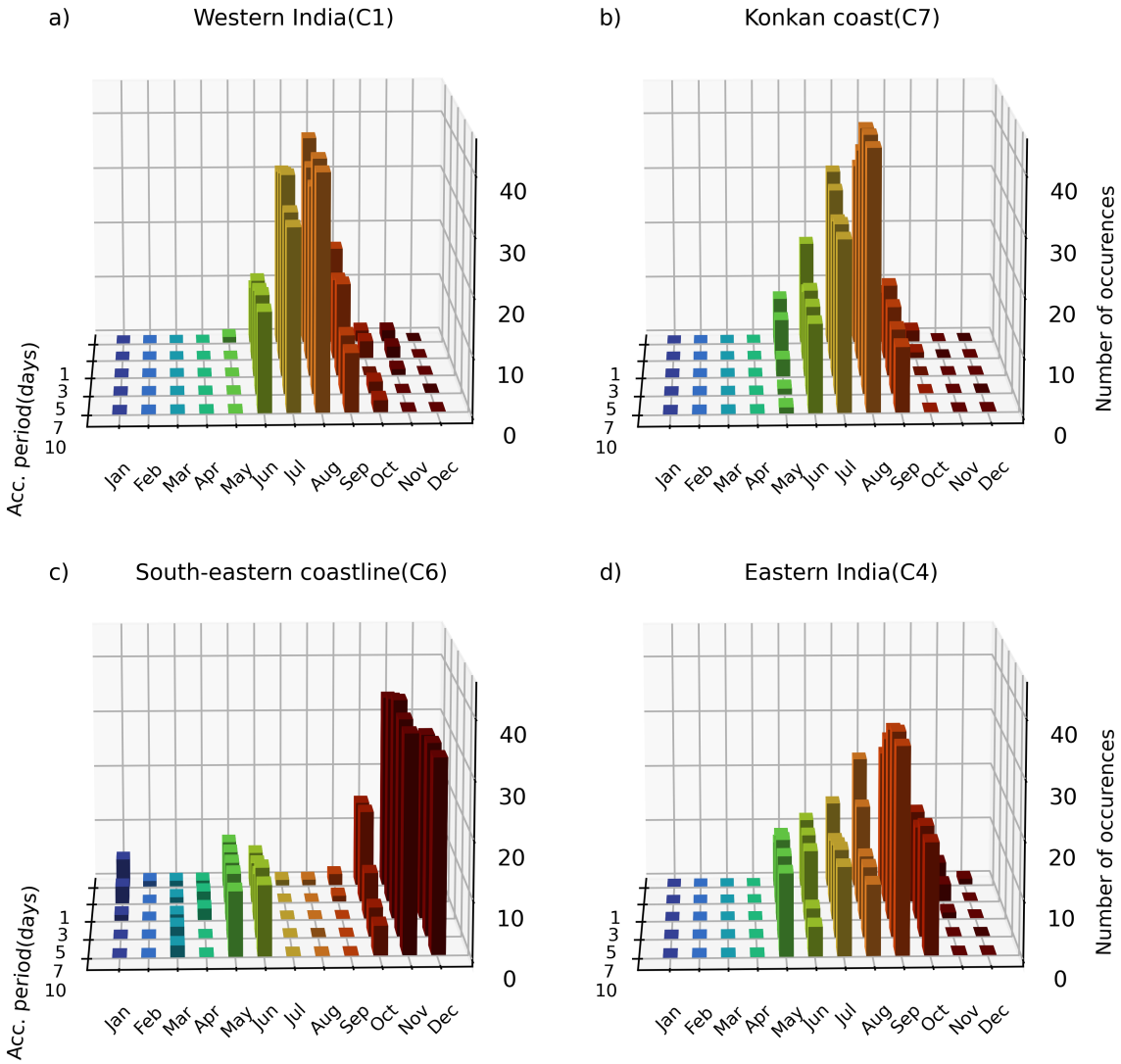

FIGURE 11 | Seasonal distribution of the first 100 events across various accumulated precipitation periods (1, 3, 5, 7, and 10 days) in four regions: (a) Western India; (b) Konkan coast; (c) South-eastern coastline; and (d) Eastern India. [Colour figure can be viewed at wileyonlinelibrary.com]

occurrences from May to October, with a significant concentration in September (Figure 11d). This pattern can be attributed to the proximity of Eastern India to the Bay of Bengal, where synoptic systems such as tropical cyclones, lows, and depressions are frequent during both the Indian summer and northeast monsoon, resulting in distinctive rainfall patterns (Soman and Kumar 1990; Khole and De 2003). For instance, approximately 10% of the world's tropical cyclones make landfall on.

3.3 | Examples of Moisture Transport Associated to Top Rank Events

The transport of moisture constitutes a critical aspect of the atmospheric branch of the water cycle, representing the main link between oceanic evaporation and continental precipitation (Gimeno et al. 2012). Numerous authors have investigated the relationship between anomalous moisture transport and precipitation extremes (Gaspar et al. 2023; Slinskey et al. 2020; Ralph et al. 2019; Ramos et al. 2015; Gimeno et al. 2016). Such events can result in devastating floods, causing significant socioeconomic impacts (Ramos et al. 2015; Slinskey et al. 2020). The linkage between anomalous atmospheric moisture transport and the occurrence of extreme precipitation and floods in India has been extensively explored in prior research (Dhana Laskhmi and Satyanarayana 2020; Lyngwa and Nayak 2021; Goyal et al. 2022; Mahto et al. 2023; Raghuvanshi and Agarwal 2023). As evidenced by the findings in the preceding sections, it is affirmed that occurrences of extreme precipitation events are prevalent throughout the Indian subcontinent, notably during the monsoon season (Sahany et al. 2018; Joseph and Sijikumar 2004; Kumar, Chanda, and Pasupuleti 2020). In this section, the characterisation of the vertically integrated horizontal water vapour transport (IVT) patterns associated with the highest-ranking event over a 10-day cumulative period was performed, in order to highlight its relevance to the analysed events. For simplicity, we focused on the most extreme events that dominated across different durations based on spatial extent and intensity, specifically those that took place on the Konkan coast in August 2019 and along the southeastern coastline in November 2018. A similar analysis for 10-day top-ranked events for the other two coastal regions, that is, over Western and Eastern India, is provided in Figures S10 and S13–S15. Figure 12 (right column) and Figure S11 illustrates the IVT fields between 30 July and 8 August 2019, corresponding to the accumulated precipitation period for the top-ranked event. A conspicuous westward flux intensifies daily, reaching values exceeding 1000 kg/m s over the main part of the Konkan coast for six consecutive days (3–8 August). This moisture transport, coupled with favourable thermodynamic conditions, played a pivotal role in precipitating the extreme rainfall observed during this period.

Upon closer examination of the corresponding thermodynamic fields (Figure 12 left column), a persistent extensive region of significant precipitation is observed, almost continuously lingering over the Konkan coast. Furthermore, from a dynamic perspective, it is evident that these high precipitation values are associated with successive frontal systems continuously traversing the Arabian Sea, exhibiting a predominant

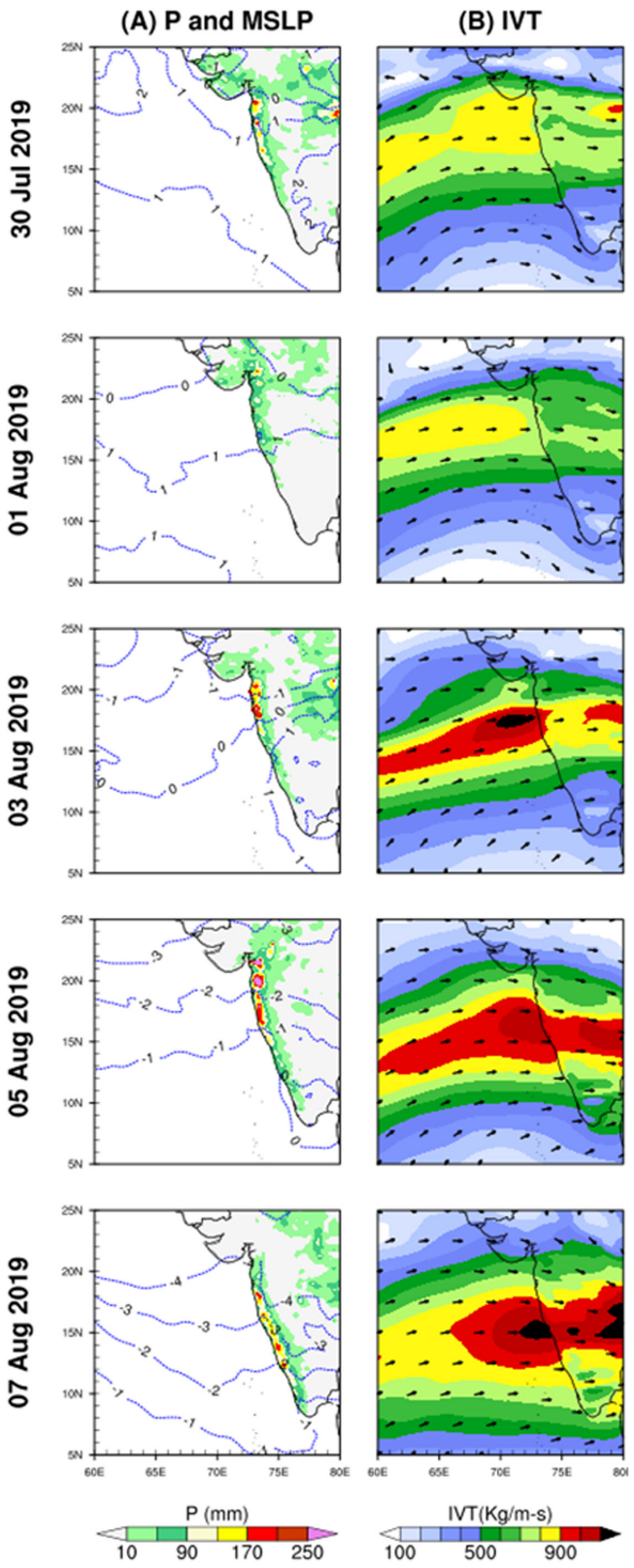

FIGURE 12 | Spatial map showing (left column) Daily precipitation (shading; units mm), and anomalies in composites of MSLP (contours; units: HPa); and (right column) Daily IVT (shading; units: Kg/m-s) over Konkan coast region during top ranked event, that is, August 2019. Black colour arrows illustrate IVT flux direction. [Colour figure can be viewed at wileyonlinelibrary.com]

southwest to northeast direction. Specifically, when a substantial amount of daily precipitation is observed in the Konkan coast (Figure 12 left column) high values of moisture transport (exceeding 900 kg/ms) can be observed over the Arabian Sea and reaching the Konkan coast (Figure 12 right column). For the South-eastern coastline, the top event is clearly linked to the passage of Cyclone "Nisha," which started in the Indian Ocean region at the end of November 2008 (Figure 13). Originating as a low-pressure system over Sri Lanka (Figure 13 left column; negative anomalies of MSLP during the days 25–27), gradually intensified into a tropical cyclonic storm. According to Srinivas et al. (2010), the tropical cyclone moved slowly, advecting a substantial amount of moisture from the sea and made landfall near Karaikal on 25 November, impacting the South-eastern coast (Figure 13 right column; Figure S12). Notably, "Nisha" remained quasi-stationary near the coast for about 24 h, causing exceptionally heavy rainfall above 200 mm (Figure 13; 25 and 26 November). A more in-depth analysis of the synoptic conditions for 27 November (the day with the highest amount of precipitation in the entire event) can be seen in Figures 13 left and S6. Thus, the top-ranked events for both the Konkan coast and South-eastern coastline events were associated with anomalous moisture transport. In the case of the Konkan coast event, the moisture transport was from the Arabian Sea, while in the case of the South-eastern coastline event, the moisture transport was associated with Cyclone "Nisha." This suggests that anomalous moisture transport is a key factor in the occurrence of extreme precipitation events in India, which is in line with the publications referred in the beginning of the section (Kumar, Chanda, and Pasupuleti 2020; Kulkarni et al. 2020; Sahany et al. 2018; Joseph and Sijikumar 2004).

4 | Conclusion

This study ranks extreme precipitation events in India across different regions (four coastal regions) and time scales (1–10 day accumulated periods) to distinguish between the distinct implications of shorter-duration heavy rainfall, which frequently causes flash flooding, and longer-duration events, which are associated with large-scale flooding and other disruptive consequences. Furthermore, this study investigates the relationship between the top-ranked extreme precipitation occurrences and atmospheric moisture transport across various areas and time scales. The results show that for each geographical region, a few extreme precipitation events dominated the top ten rankings across numerous time scales, showing that the detected extreme precipitation events are persistent in nature and severity. In addition, this study demonstrated the robustness of the methodology used to detect and rank multi-day exceptional precipitation events, creating a detailed database identifying extreme precipitation events across multiple temporal and spatial specifications. Analysis of seasonal patterns shows that these events occur during both the Indian Summer Monsoon (ISM) and the North-East Monsoon (NEM), underscoring their occurrence throughout the year. Furthermore, the results show that the spatiotemporal dynamics and characteristics of atmospheric moisture transport have a considerable influence on the occurrence of extreme precipitation events. Overall, the findings of this study provide sufficient context and insight to aid in forecasting atmospheric moisture transport-linked extreme precipitation occurrences

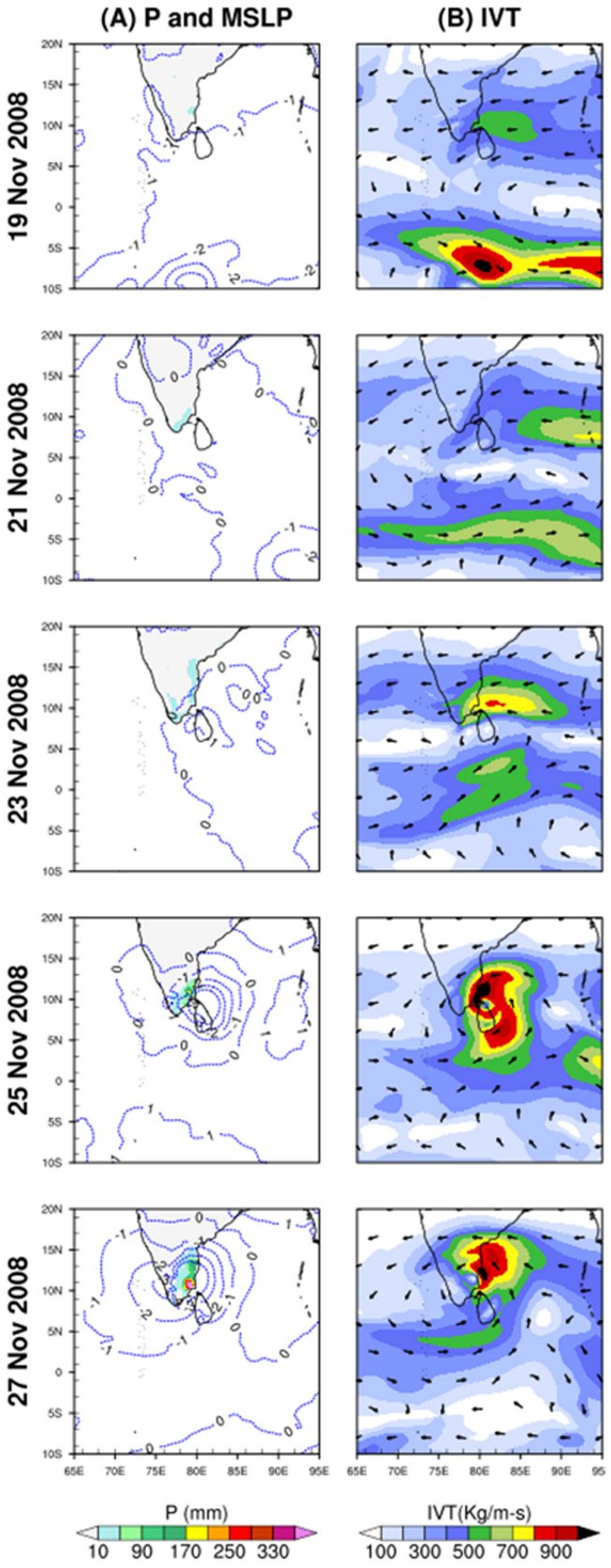

FIGURE 13 | Spatial map showing (left column) Daily precipitation (shading; units mm), and anomalies in composites of MSLP (contours; units: hPa); and (right) Daily IVT (shading; units: Kg/m-s) over South eastern coast region during top ranked event, that is, November 2008. Black colour arrows illustrate IVT flux direction. [Colour figure can be viewed at wileyonlinelibrary.com]

across the Indian subcontinent. Moreover, the synoptic patterns highlighted in this work can be used to develop early warning systems for heavy precipitation-driven floods in India. To fill certain information gaps, future research could look into the impact of the persistence of several additional synoptic meteorological parameters (wind speed, relative humidity, etc., at various tropospheric levels) on extreme precipitation characteristics.

Author Contributions

T. H. Gaspar: conceptualization, investigation, writing – original draft, methodology, validation, visualization, software, formal analysis, data curation, resources. **R. M. Trigo:** funding acquisition, supervision, project administration, writing – review and editing, conceptualization, validation, investigation, writing – original draft, methodology. **A. M. Ramos:** writing – review and editing, supervision, conceptualization, validation, funding acquisition, methodology. **A. S. Raghuvanshi:** writing – review and editing, conceptualization, validation, formal analysis, investigation, writing – original draft, methodology. **A. Russo:** writing – review and editing, supervision, validation. **P. M. M. Soares:** writing – review and editing, supervision, validation. **T. M. Ferreira:** writing – review and editing. **A. Agarwal:** conceptualization, writing – review and editing, supervision, funding acquisition, validation, methodology, investigation, project administration, writing – original draft.

Acknowledgements

Authors greatly appreciate the data provided by the India Meteorological Department (IMD). A. Russo also acknowledges the Portuguese Fundação para a Ciência e a Tecnologia (FCT) I.P./MCTES for project COMPLEX (https://doi.org/10.54499/2022.01167.CEECIND/CP1722/CT0006). A. M. Ramos was supported by the Helmholtz 'Changing Earth—Sustaining our Future' program.

Conflicts of Interest

The authors declare no conflicts of interest.

Data Availability Statement

The data that support the findings of this study are available from the corresponding author upon reasonable request.

References

Ali, H., V. Mishra, and D. S. Pai. 2014. "Observed and Projected Urban Extreme Rainfall Events in India." *Journal of Geophysical Research: Atmospheres* 119: 12621–12641. https://doi.org/10.1002/2014jd022264.

Beguería, S., S. M. Vicente-Serrano, J. I. López-Moreno, and J. M. García-Ruiz. 2009. "Annual and Seasonal Mapping of Peak Intensity, Magnitude and Duration of Extreme Precipitation Events Across a Climatic Gradient, Northeast Spain." *International Journal of Climatology* 29: 1759–1779. https://doi.org/10.1002/joc.1808.

Bharath, R., and V. V. Srinivas. 2014. "Regionalization of Extreme Rainfall in India." *International Journal of Climatology* 35: 1142–1156. https://doi.org/10.1002/joc.4044.

Cadet, D. L., and S. Greco. 1987. "Water Vapor Transport over the Indian Ocean during the 1979 Summer Monsoon. Part II: Water Vapor Budgets." *Monthly Weather Review* 115: 2358–2366. https://doi.org/10.1175/1520-0493.

De, U. S., R. K. Dube, and G. S. Prakasa Rao. 2005. "Extreme Weather Events Over India in the Last 100 Years." *Journal of Indian Geophysical Union* 9, no. 3: 173–187.

Dube, A., R. Ashrit, S. Kumar, and A. Mamgain. 2020. "Improvements in Tropical Cyclone Forecasting Through Ensemble Prediction System at Ncmrwf in India." *Tropical Cyclone Research and Review* 9, no. 2: 106–116.

Dullaart, J., S. Muis, N. Bloemendaal, M. Chertova, A. Couasnon, and H. Aerts. 2021. "Accounting for Tropical Cyclones More Than Doubles the Global Population Exposed to Low-Probability Coastal Flooding." *Communications Earth & Environment* 2: 1–11. https://doi.org/10.1038/s43247-021-00204-9.

Gaspar, T., A. M. Ramos, R. Deus, P. J. Pinto, and R. M. Trigo. 2023. "The Impact of Multiple Atmospheric Rivers on the Extreme Precipitation Events in December 2022 in Portugal." *Meteorology and Geophysics* 52: 52–59.

Gimeno, L., A. Stohl, R. M. Trigo, et al. 2012. "Oceanic and Terrestrial Sources of Continental Precipitation." *Reviews of Geophysics* 50, no. 4: 1–41.

Gimeno, L., F. Dominguez, R. Nieto, et al. 2016. "Major Mechanisms of Atmospheric Moisture Transport and Their Role in Extreme Precipitation Events." *Annual Review of Environment and Resources* 41: 117–141.

Gupta, K. 2007. "Urban Flood Resilience Planning and Management and Lessons for the Future: A Case Study of Mumbai, India." *Urban Water Journal* 4, no. 3: 183–194. https://doi.org/10.1080/15730620701464141.

Goswami, B. N., V. Venugopal, D. Sengupta, M. S. Madhusoodanan, and P. K. Xavier. 2006. "Increasing Trend of Extreme Rain Events Over India in a Warming Environment." *Science* 314: 1442–1445. https://doi.org/10.1126/science.1132027.

Goyal, M. K., A. K. Gupta, S. Jha, S. Rakkasagi, and V. Jain. 2022. "Climate Change Impact on Precipitation Extremes Over Indian Cities: Non-Stationary Analysis." *Technological Forecasting and Social Change* 180: 121685. https://doi.org/10.1016/j.techfore.2022.121685.

Guhathakurta, P., M. Rajeevan, D. R. Sikka, and A. Tyagi. 2014. "Observed Changes in Southwest Monsoon Rainfall Over India During 1901–2011." *International Journal of Climatology* 35: 1881–1898. https://doi.org/10.1002/joc.4095.

Guntu, R. K., R. Maheswaran, A. Agarwal, and V. P. Singh. 2020. "Accounting for Temporal Variability for Improved Precipitation Regionalization Based on Self-Organizing Map Coupled With Information Theory." *Journal of Hydrology* 590: 125236. https://doi.org/10.1016/j.jhydrol.2020.125236.

Hersbach, H., B. Bell, P. Berrisford, et al. 2020. "The ERA5 Global Reanalysis." *Quarterly Journal of the Royal Meteorological Society* 146: 1999–2049. https://doi.org/10.1002/qj.3803.

Joseph, P. V., and S. Sijikumar. 2004. "Intraseasonal Variability of the Low-Level Jet Stream of the Asian Summer Monsoon." *Journal of Climate* 17: 1449–1458. https://doi.org/10.1175/1520-0442(2004)017<1449:ivotlj>2.0.co;2.

Khole, M., and U. S. De. 2003. "A Study on North-East Monsoon Rainfall Over India." *Mausam* 54: 419–426. https://doi.org/10.54302/mausam.v54i2.1527.

Kulkarni, A., T. P. Sabin, J. S. Chowdary, et al. 2020. "Precipitation Changes in India." In *Assessment of Climate Change Over the Indian Region*, edited by R. Krishnan, J. Sanjay, C. Gnanaseelan, M. Mujumdar, A. Kulkarni, and S. Chakraborty. Singapore: Springer. https://doi.org/10.1007/978-981-15-4327-2_3.

Kumar, S., K. Chanda, and S. Pasupuleti. 2020. "Spatiotemporal Analysis of Extreme Indices Derived From Daily Precipitation and Temperature for Climate Change Detection Over India." *Theoretical and Applied Climatology* 140: 343–357. https://doi.org/10.1007/s00704-020-03088-5.

Kurths, J., A. Agarwal, R. Shukla, et al. 2019. "Unravelling the Spatial Diversity of Indian Precipitation Teleconnections via a Non-Linear

Multi-Scale Approach." *Nonlinear Processes in Geophysics* 26: 251–266. https://doi.org/10.5194/npg-26-251-2019.

Laskhmi, D. D., and A. N. V. Satyanarayana. 2020. "Climatology of Landfalling Atmospheric Rivers and Associated Heavy Precipitation Over the Indian Coastal Regions." *International Journal of Climatology* 40: 5616–5633. https://doi.org/10.1002/joc.6540.

Lavers, D. A., G. Villarini, R. P. Allan, E. F. Wood, and A. J. Wade. 2012. "The Detection of Atmospheric Rivers in Atmospheric Reanalyses and Their Links to British Winter Floods and the Large-Scale Climatic Circulation." *Journal of Geophysical Research: Atmospheres* 117. https://doi.org/10.1029/2012jd018027.

Lyngwa, R. V., and M. A. Nayak. 2021. "Atmospheric River Linked to Extreme Rainfall Events Over Kerala in August 2018." *Atmospheric Research* 253: 105488. https://doi.org/10.1016/j.atmosres.2021.105488.

Mahto, S. S., M. A. Nayak, D. P. Lettenmaier, and V. Mishra. 2023. "Atmospheric Rivers That Make Landfall in India Are Associated With Flooding." *Communications Earth & Environment* 4: 4. https://doi.org/10.1038/s43247-023-00775-9.

Mannan, A., S. Chaudhary, C. T. Dhanya, and A. K. Swamy. 2017. "Regionalization of Rainfall Characteristics in India Incorporating Climatic Variables and Using Self-Organizing Maps." *ISH Journal of Hydraulic Engineering* 24: 147–156. https://doi.org/10.1080/09715010.2017.1400409.

Mishra, A. K., V. Nagaraju, M. Rafiq, and S. Chandra. 2018. "Evidence of Links Between Regional Climate Change and Precipitation Extremes Over India." *Weather* 74: 218–221. https://doi.org/10.1002/wea.3259.

Mishra, V., and H. L. Shah. 2018. "Hydroclimatological Perspective of the Kerala Flood of 2018." *Journal of the Geological Society of India* 92: 645–650. https://doi.org/10.1007/s12594-018-1079-3.

Mukherjee, S., and A. K. Mishra. 2021. "Increase in Compound Drought and Heatwaves in a Warming World." *Geophysical Research Letters* 48: 1. https://doi.org/10.1029/2020gl090617.

Murty, T. S., R. A. Flather, and R. F. Henry. 1986. "The Storm Surge Problem in the Bay of Bengal." *Progress in Oceanography* 16: 195–233. https://doi.org/10.1016/0079-6611(86)90039-x.

Neiman, P. J., F. Martin Ralph, G. A. Wick, J. D. Lundquist, and M. D. Dettinger. 2008. "Meteorological Characteristics and Overland Precipitation Impacts of Atmospheric Rivers Affecting the West Coast of North America Based on Eight Years of SSM/I Satellite Observations." *Journal of Hydrometeorology* 9, no. 1: 22–47.

Pai, D. S., M. Rajeevan, O. P. Sreejith, B. Mukhopadhyay, and N. S. Satbha. 2014. "Development of a New High Spatial Resolution (0.25 ×0.25) Long Period (1901–2010) Daily Gridded Rainfall Data Set Over India and Its Comparison With Existing Data Sets Over the Region." *Mausam* 65, no. 1: 1–18.

Pai, D. S., M. Rajeevan, O. P. Sreejith, B. Mukhopadhyay, and N. S. Satbha. 2021. "Development of a New High Spatial Resolution (0.25° ×0.25°) Long Period (1901–2010) Daily Gridded Rainfall Data Set Over India and Its Comparison With Existing Data Sets Over the Region." *Mausam* 65: 1–18. https://doi.org/10.54302/mausam.v65i1.851.

Patil, N., C. Venkataraman, K. Muduchuru, S. Ghosh, and A. Mondal. 2018. "Disentangling Sea-Surface Temperature and Anthropogenic Aerosol Influences on Recent Trends in South Asian Monsoon Rainfall." *Climate Dynamics* 52: 2287–2302. https://doi.org/10.1007/s00382-018-4251-y.

Payne, A. E., and G. Magnusdottir. 2014. "Dynamics of Landfalling Atmospheric Rivers Over the North Pacific in 30 Years of Merra Reanalysis." *Journal of Climate* 27, no. 18: 7133–7150.

Raghuvanshi, A. S., and A. Agarwal. 2023. "Unraveling Atmospheric Moisture Transport Linkages to Extreme Precipitation Events and Associated Synoptic Features Over India." *Journal of Hydrology* 626: 130290. https://doi.org/10.1016/j.jhydrol.2023.130290.

Raghuvanshi, A. S., and A. Agarwal. 2024. "Multiscale Dynamics of Transient Merging Between Western Disturbances and Monsoonal Lows: Connections to the July 2023 Flood in Himachal Pradesh." *Atmospheric Research* 304: 107401. https://doi.org/10.1016/j.atmosres.2024.107401.

Raghuvanshi, A. S., R. M. Trigo, and A. Agarwal. 2025. "Climatology of Extreme Precipitation Spells Induced by Cloudburst-Like Events During the Indian Summer Monsoon." *Journal of Hydrology X* 26: 100197. https://doi.org/10.1016/j.hydroa.2024.100197.

Raj, S., R. Shukla, R. M. Trigo, et al. 2021. "Ranking and Characterization of Precipitation Extremes for the Past 113 Years for Indian Western Himalayas." *International Journal of Climatology* 41: 6602–6615. https://doi.org/10.1002/joc.7215.

Rajeevan, M., C. K. Unnikrishnan, K. Jyoti Bhate, N. Kumar, and P. P. Sreekala. 2012. "Northeast Monsoon Over India: Variability and Prediction." *Meteorological Applications* 19: 226–236. https://doi.org/10.1002/met.1322.

Ralph, F. M., J. J. Rutz, J. M. Cordeira, et al. 2019. "A Scale to Characterize the Strength and Impacts of Atmospheric Rivers." *Bulletin of the American Meteorological Society* 100: 269–289. https://doi.org/10.1175/bams-d-18-0023.1.

Ramos, A. M., M. J. Martins, R. Tomé, and R. M. Trigo. 2018. "Extreme Precipitation Events in Summer in the Iberian Peninsula and Its Relationship With Atmospheric Rivers." *Frontiers in Earth Science* 6: 8. https://doi.org/10.3389/feart.2018.00110.

Ramos, A. M., R. M. Trigo, and M. L. R. Liberato. 2016. "Ranking of Multi-Day Extreme Precipitation Events Over the Iberian Peninsula." *International Journal of Climatology* 37: 607–620. https://doi.org/10.1002/joc.4726.

Ramos, A. M., R. M. Trigo, M. L. R. Liberato, and R. Tome. 2015. "Daily Precipitation Extreme Events in the Iberian Peninsula and Its Association With Atmospheric Rivers*." *Journal of Hydrometeorology* 16: 579–597. https://doi.org/10.1175/jhm-d-14-0103.1.

Ranger, N., S. Hallegatte, S. Bhattacharya, et al. 2010. "An Assessment of the Potential Impact of Climate Change on Flood Risk in Mumbai." *Climatic Change* 104: 139–167. https://doi.org/10.1007/s10584-010-9979-2.

Sahany, S., S. K. Mishra, R. Pathak, and B. Rajagopalan. 2018. "Spatiotemporal Variability of Seasonality of Rainfall Over India." *Geophysical Research Letters* 45, no. 14: 7140–7147.

Singh, O. P., T. M. Ali Khan, and M. S. Rahman. 2000. "Changes in the Frequency of Tropical Cyclones Over the North Indian Ocean." *Meteorology and Atmospheric Physics* 75: 11–20. https://doi.org/10.1007/s007030070011.

Slinskey, E. A., P. C. Loikith, D. E. Waliser, B. Guan, and A. Martin. 2020. "A Climatology of Atmospheric Rivers and Associated Precipitation for the Seven Us National Climate Assessment Regions." *Journal of Hydrometeorology* 21: 1–55. https://doi.org/10.1175/jhm-d-20-0039.1.

Soman, M. K., and K. K. Kumar. 1990. "Some Aspects of Daily Rainfall Distribution Over India During the South-West Monsoon Season." *International Journal of Climatology* 10: 299–311. https://doi.org/10.1002/joc.3370100307.

Sorí, R., L. Gimeno-Sotelo, R. Raquel Nieto, et al. 2023. "Oceanic and Terrestrial Origin of Precipitation Over 50 Major World River Basins: Implications for the Occurrence of Drought." *Science of the Total Environment* 859: 160288. https://doi.org/10.1016/j.scitotenv.2022.160288.

Srinivas, C. V., V. Yesubabu, R. Venkatesan, and S. S. V. S. Ramarkrishna. 2010. "Impact of Assimilation of Conventional and Satellite Meteorological Observations on the Numerical Simulation of a Bay of Bengal Tropical Cyclone of November 2008 Near Tamilnadu Using Wrf Model." *Meteorology and Atmospheric Physics* 110: 19–44. https://doi.org/10.1007/s00703-010-0102-z.

Vijaykumar, P., S. Abhilash, A. V. Sreenath, et al. 2021. "Kerala Floods in Consecutive Years—Its Association With Mesoscale Cloudburst and Structural Changes in Monsoon Clouds Over the West Coast of India." *Weather and Climate Extremes* 33: 100339. https://doi.org/10.1016/j.wace.2021.100339.

Vinnarasi, R., and C. T. Dhanya. 2016. "Changing Characteristics of Extreme Wet and Dry Spells of Indian Monsoon Rainfall." *Journal of Geophysical Research: Atmospheres* 121: 2146–2160. https://doi.org/10.1002/2015jd024310.

Zhou, T.-J., and Y. Ru-Cong. 2005. "Atmospheric Water Vapor Transport Associated With Typical Anomalous Summer Rainfall Patterns in China." *Journal of Geophysical Research: Atmospheres* 110, no. D8: 1–10.

Supporting Information

Additional supporting information can be found online in the Supporting Information section.